Mesenchymal stem cell interacted with PLCL braided scaffold coated with poly- l -lysine/hyaluronic acid for ligament tissue engineering

Xing Liu, Cédric Laurent, Qiaoyue Du, Laurie Targa, Ghislaine Cauchois, Yun Chen, Xiong Wang, Natalia de Isla

Mesenchymal stem cell interacted with PLCL braided scaffold coated with Poly-L-lysine/Hyaluronic Acid for Ligament tissue engineering

Xing Liu[1], Cédric Laurent[2], Qiaoyue Du[3], Laurie Targa[1],Ghislaine Cauchois[1], Yun Chen[3], Xiong Wang[1], Natalia de Isla[1]

[1]*CNRS UMR 7365 -Université de Lorraine, Ingénierie Moléculaire et Physiopathologie Articulaire (IMoPA), Vandœuvre-lès-Nancy, France*

[2]*CNRS UMR 7239 LEM3 - Université de Lorraine, Vandoeuvre-lès-Nancy, France*

[3]*Department of Biomedical Engineering, School of Basic Medical Science, Wuhan University, Wuhan,China*

Correspondence to: xing.liu@univ-lorraine.fr; natalia.de-isla@univ-lorraine.fr

Abstract: The challenge of finding an adapted scaffold for ligament tissue engineering still remains unsolved after years of researches. A technology to fabricate a multilayer braided scaffold with flexible and elastic Poly (L-lactide-co-caprolactone) (PLCL 85/15) has been recently pioneered by our team. In the present study, polyelectrolyte multilayer films (PEM) with poly-L-lysine (PLL)/ hyaluronic acid (HA) were deposited on this scaffold. After PEM modification, polygonal (PLL) and particle-like (HA) structures were present on the braided scaffold with no significant variation of fibers Young's modulus. Wharton's Jelly Mesenchymal Stem Cells (WJ-MSC) and Bone Marrow Mesenchymal Stem Cells (BM-MSC) showed good metabolic activity on scaffolds. They presented a spindled shape along the fiber longitudinal direction, and crossed the fibers to form cell bridges. Collagen type I, collagen type III and tenascin-C secreted by MSCs were detected on day 14. Moreover, one-layer modified scaffold presented increased chemotaxis. As a conclusion, our results indicate that this braided PLCL scaffold with one layer PEM modification shows inspiring potential with satisfying mechanical properties and

biocompatibility. It opens new perspectives to incorporate growth factors within PEM-modified braided PLCL scaffold for ligament tissue engineering and to recruit endogenous cells after implantation.

Keyword: Poly (L-lactide-co-caprolactone), braided scaffold, mesenchymal stem cell, polyelectrolyte multilayer films, ligament tissue engineering

Introduction

Ligament injuries are among the highest incidence of musculoskeletal disorders,[1-4] especially for the people who commonly do sports, rigorous physical activities, suffer acute trauma, or for aged people. The main strategy for repairing injured ligament consists in a surgical intervention called ligamentoplasty. Grafts[5–7] used in such interventions include autografts, allografts, and artificial substitutes. These therapies are subject to constant improvements,[5,8] resulting in the increase of joint stability, recovered mechanical properties, and patients' overall satisfaction. However, such surgeries are still associated with drawbacks[9,10] including donor site morbidity, immune rejection, or limited graft sources. With the rise of tissue engineering, ligament tissue engineering could constitute a novel, attractive and alternative approach to recover the function of injured ligament.[1, 3, 7]

Scaffolds with the architectures of sponges, knitted fibers, meshes, hydrogels, wired yarns, and braided fibers have already been reported[3, 11, 12] in ligament tissue engineering. Despite their benefits, they also suffer from some drawbacks, [3, 12, 13] such

as insufficient mechanical properties, brittle behavior, or lack of functional groups for molecular signaling. In our previous studies,[14, 15] PLCL has been used to develop a novel multilayer braided scaffold. It presents a porous structure for cell or tissue ingrowth, nutrient exchange, and post-graft degradation. Thanks to the adjustable geometrical parameters of this architecture (e.g. number of layers, fiber diameter and braiding angle), the mechanical strength could also be adjusted to fulfill requirements of different ligaments. PLCL is a synthetic biodegradable co-polymer with high elasticity consisting of polylactide (PLLA) and polycaprolactone (PCL). It has already been pointed out[16] to support tendon cell proliferation, and has been widely applied in tissue engineering because of its good biocompatibility and mechanical properties.

Seeding cells[17–19] could also contribute to the functionality of tissue engineered constructs by encouraging its colonization and extra cellular matrix (ECM) synthesis. Ligament fibroblasts[19] may appear as natural candidate reparative cells for ligament tissue engineering, but there are limited by cell availability, quantity of donors and also differentiation capacity. Because of self-renew ability, differentiation potential, and bioactive molecule secretion activity, Mesenchymal Stem Cells (MSCs) have become a popular cell source applied in tissue engineering.[17, 20] In addition, MSCs have already been reported[17, 20] to proliferate better and produce more collagen than fibroblasts. Wharton's Jelly Mesenchymal Stem Cells (WJ-MSC) and Bone Marrow Mesenchymal Stem Cells (BM-MSC) were thus selected as cell sources in our present study.

In the last decades, Layer-By-Layer (LBL) technology has been widely used to modify the surface of biomaterials in order to improve the integration or add specialized properties to scaffolds.[21, 22] Examples of LBL biological applications include mediation of cellular functions to promote cell adhesion, proliferation, differentiation; biosensors; drugs or bioactive molecular delivery system, and biomimetics. The cellular adhesion and homogeneous cell distribution on the scaffold is a primary element in tissue engineering, and many studies[7, 23] have emphasized the importance of growth factors to promote MSCs attachment, proliferation, and matrix synthesis in the process of ligament/tendon repair. In the light of the advantages of LBL technology for cell adhesion, and the demand of growth factor delivery system for tissue engineering, LBL modification was introduced in our study in order to promote a ligamentous tissue. Poly-L-lysine (PLL) and Hyaluronic Acid (HA) were selected[24, 25] as polycation and polyanion for PEM. HA, as a component of extracellular matrix, plays an important role in improving cell growth, differentiation and migration, but it has been observed to be non-adhesive to cells.[24, 26] On the contrary, PLL has been shown[27,28] to promote cell adhesion and it has widely been used for biomaterial coating and drug delivery. The pair of PLL/HA PEM was expected to be an effective system to improve MSCs behavior on scaffolds.

Prior to any incorporation of growth factors into a LBL-treated scaffold, it is crucial to study the effect of PLL/HA LBL modification on the behaviors of WJ-MSC and BM-MSC on PLCL braided scaffold. Therefore, in the present contribution the effect

of LBL technology on MSCs proliferation, distribution, morphology, collagen synthesis, tenascin-C expression and migration were evaluated, as well the consequence of this treatment on scaffold topology, and mechanical properties.

METHODS AND MATERIALS

Scaffold fabrication

PLCL (85/15) braided scaffold was fabricated according to previously described methods.[14, 15] Briefly, it consists of a multilayer braided structure, each layer being made up of 16 fibers of poly(lactide-co-ε-caprolactone) (PLCL, Purac Biomaterials) with a lactic acid/ε-caprolactone proportion of 85/15. The polymer was firstly processed into 170 μm fibers using a homemade extrusion machine at 180°C. Fibers were collected on bobbins, and 16 bobbins were installed on a maypole braiding machine (Composite & Wire Machinery, United States) to form braided scaffolds. Six layers were superposed in total, for a resulting scaffold of 96 fibers measuring around 4mm in diameter.

Scaffold modification with LBL technology

PLL (Sigma) and HA (Acros) were dissolved in the NaCl-Tris buffer (pH6.3) at a concentration of 1 mg/mL respectively. Scaffolds were cut into 1 cm-long parts. Firstly, scaffolds were immersed into PLL solutions for 7 min, then gently rinsed in NaCl-Tris buffer for 1 min. They were subsequently introduced into HA solution for 7 min, and then rinsed. Scaffold-blank (SB) refers to the scaffold without LBL modification; scaffold-PLL (SP) refers to scaffold modified only by PLL solution, and scaffold-PLL-HA-PLL（S1L）refers to one-layer modification. This configuration

(pH6.3 and only one-layer modification) was selected based on preliminary studies briefly reported in supplementary material.

Scaffold characterization

Characterization of scaffold by Fourier Transform Infrared Spectroscopy (FTIR)

PLCL fibers were vacuum-dried at 60°C for 24 h, and cut into fine powders for the measurements by FTIR. The dry powders were mixed with Potassium bromide (KBr), and spectra were recorded on an FTIR spectrometer (Nicolet, USA) over the wavenumber range from 4000 to 600 cm^{-1}.

Detecting of PLL/HA coating by Atomic Force Microscopy (AFM) and Confocal Laser Scanning Microscopy (CLSM)

The surface of modified fibers was characterized by AFM (Oxford instruments). PLCL fibers were cut into 1 cm and maintained on a glass slide. Surface topology was observed and recorded in contact mode.

PLL-FITC (Sigma) was used to replace PLL in PLL/HA system. Fibers were immersed in PLL-FITC/HA solution using the procedure described above, then detected by CLSM (Nikon).

Scaffold morphology by Scanning Electronic Microscopy (SEM)

Scaffolds were frozen with liquid nitrogen for 10 min, dried with vacuum oven for 7 h, then coated with gold and observed by SEM (TESCAN, Czech).

Mechanical properties of fibers

The mechanical properties of PLCL fibers were assessed using tensile tests performed

with a Zwick Roell 2.5 device (Zwick, Germany), at a tensile speed of 0.1mm.s^{-1}. Six 10 cm-long fibers were tested in parallel for SB, SP and S1L (n=4). The following loading cycle was prescribed 1)1% strain then unloading 2) 3% strain then unloading 3) increasing strain up to failure. Young's modulus was measured for each sample from the slope of the stress-strain curve just after the first unloading cycle (at 1% of strain).

Mesenchymal Stem Cell isolation and expansion

Human bone marrow and human umbilical cords were supplied by CHRU Hospital and Maternity Hospital (Nancy, France) with the informed consent of donors. Firstly, 25 mL α-MEM (Lonza) medium containing 10% fetal calf serum (FCS, Dominique Dutscher), 2 mM L-glutamine (Sigma), 100 U/mL penicillin /streptomycin (Gibco) and 1 µg/mL amphoterin B (Gibco) was added to 20 mL bone marrow, and centrifuged 300g for 5 min. The supernatant was removed, and cells were seeded on tissue culture plates at the density of 5×10^4 cells/cm^2, and then incubated in 37°C, 5% CO_2, 90% humidity until the cells reach 70% - 80% confluence.

Human umbilical cord was washed with 70% ethanol and cut into 3-4 cm long samples in the HBSS buffer. The cord was opened to peel off two arteries and one vein; the jelly was torn off from cordon and cut into fine pieces in HBSS buffer. After 7 days, jelly was removed, and the culture medium was changed twice a week until the cells reach 70% - 80% confluence. All MSCs used for assays were in passage 3 (P3). Before seeding cells on scaffolds, the quality of MSCs was controlled by testing biological properties as CFU test, senescence test and phenotype characterization. (data shown in

supplementary material)

MSC culture on scaffold

Firstly, scaffolds were immersed in ethanol for 30 min, then sterilized with UV for 30 min. MSCs were distributed on scaffold (3×10^5 cells, 50 μL/scaffold). MSC-scaffolds were kept in incubator for 30 min, then supplied with 0.95 mL α-MEM complete medium including 100 μg/mL ascorbic acid (Sigma) and cultured for two weeks.

Evaluation of cell biocompatibility on the scaffolds

Cell metabolic activity of MSCs on scaffold

Alamar Blue (AB) tests were performed on day 1, 3, 5, and 7. 1 mL 10% AB work solution (Thermo Fish scientific) was added to each scaffold, and incubated for 4 h. The absorbance was measured at 570 nm and 600 nm (n=3). Negative control was AB working. The percentage of Alamar Blue Reagent reduction was calculated according to manufacturer's instructions.

Cell morphology and distribution on scaffold

Scanning Electronic Microscopy (SEM)

MSC-Scaffolds were firstly fixed with 2.5% glutaraldehyde at 4°C overnight on day 14, then washed with PBS three times. MSC-scaffolds were frozen with liquid nitrogen for 10 min, dried with vacuum oven for 7 h, and then images were taken by SEM.

Confocal microscopy

Firstly, MSC-scaffolds were fixed with 1% paraformaldehyde for 10 min at room

temperature, then washed with PBS three times. Permibilization treatment was performed by adding 1 mL 0.5% triton-PBS to each well for 20 min and washed with PBS three times. 250 µL Alexa 488 Phalloidin (Life technologies) solution was supplied to each MSC-scaffold for 45 min, then washed with PBS three times. 200 µL DAPI (1/2000) (Sigma) was added to each scaffold for 15 min, and washed with PBS three times. Images were taken by confocal microscopy (Leica SP5-CFS).

Quantification of cell nuclear elongation was performed by Image J software version 1.51k. The length was defined as the longest distance through nucleus and the width was defined as the distance perpendicular to the length. Cell nuclear aspect ratio was calculated by dividing the length to the width. The area of cell nucleus ($n \geq 100$ from more than three images) was measured by Image J 1.51k.

Extracellular matrix synthesized by MSCs on scaffold

After 2 weeks, MSC-scaffolds were firstly fixed with 1% paraformaldehyde for 10 min, then washed with PBS three times. 5% PBS-BSA blocking buffer was added to scaffolds for 30 min. The first antibody anti-collagen type I (CALBIOCHEM), collagen type III (Sigma) and anti-tenascin-C (Abcam) were added (250 µL) to scaffolds for 1 h, then washed with PBS three times. The second antibody anti-Rabbit IgG-Alexa488 (1/50) (Life technologies) and anti-mouse IgG-Alexa488 were distributed (250 µL) to scaffold for 45 min, then washed with PBS three times. 200 µL DAPI (1/2000) was added to each scaffold for 15 min. MSC-Scaffolds were washed with PBS three times, and observed by fluorescence microscopy. Negative controls

were performed as MSC with only second antibody, and positive controls were tested as fibroblast with anti-collagen I , collagen III and tenascin-c and second antibody (data shown in supplementary material).

Cell Chemotactic assay

PLCL films were fabricated by hot-processing method, and modified with PLL/HA PEM as PLCL braided scaffold treatment. Boyden chamber assay was performed for migration test by using a transwell (Corning® FluoroBlok™) with 0.8 μm pore fluorescence blocking PET track-etched membrane insert according to manufacturer's instructions. The downside of insert was coated with 100 μL collagen for 30 min. MSCs were starved 24 h before cell migration assay. SB, SP, and S1L film with 500 μL α-MEM complete medium were introduced to each reservoir. 1.5×10^5 cell suspension in α-MEM without FCS (200 μL) was added into each insert. After 24 h, cells were stained with calcein AM (Thermo Fish scientific) (1/1000) for 30 min, then washed with PBS three times. Cell distribution was observed by fluorescence microscopy and fluorescence intensity was measured by fluorescence spectrophotometer.

RESULTS

Physiochemical properties of PLCL braided scaffold with/without PLL/HA modification

Fourier-transform infrared spectroscopy of PLL/HA LBL modification

The structure of PLCL fiber with/without PLL/HA modification are shown in Fig.1 by FTIR. The spectra at 2990 cm^{-1} (PLLA), 2945 cm^{-1} (PLLA) and 2860 (PCL) cm^{-1} demonstrated[29] the presence of alkyl group of copolymer PLCL. Bands at 1130 cm^{-1} and 1065 cm^{-1} corresponded to ester backbone of PLA in scaffold SP and S1L respectively.[30] The wavelength of PLL in SP was present as anion group[31] at 1600 cm^{-1}. The wavelength of HA in PLL/HA-PLL was present as carboxylate anion group[31] at 1616 cm^{-1} and 1413 cm^{-1}. The wavelength of amine groups of PLL[31] was shown at 1630 cm^{-1} in PLL/HA-PLL.

Topology of PLL/HA LBL modification.

PLL-FITC was observed to cover the fiber homogeneously by CLSM (Fig.2a), and from SP to S1L the fluorescence intensity was increased. As shown in Fig.2b, the surface of fiber was globally flat and smooth. Irregular polygonal structures on the surface of SP were deduced to correspond to PLL molecules, while the “particles” structures on S1L were attributed to HA molecules by AFM.

Morphology of scaffold

SEM images of PLCL braided scaffold in Fig.3a indicated a porous and braided structure, and this multilayer structure was not influenced by PLL/HA modification. For SB (scaffold without modification), the fibers kept the same texture from original fabrication, while for SP and S1L the fibers presented a relatively smooth surface after modification. The architecture of this multi-layer braided scaffold is illustrated in

Fig.3b: the scaffold was composed with six layers shown in six different colors (16 braided fibers each layer).

Mechanical properties

Typical stress-strain curves as well as Young's modulus evolution are exhibited in Fig.4. Young's modulus of SB,SP and S1L were respectively 1616 ± 643 MPa, 1608 ± 156 MPa and 1758 ± 470 MPa. No significant changes in Young's modulus were therefore observed. The three types of fibers broke for a strain around 15-25% with no significant effect of surface modification.

Biocompatibility of MSC-scaffold in vitro

MSC metabolic activity on scaffold

Cell metabolic activity was detected by AB and is presented in Fig.5. The metabolic activity of WJ-MSC on SB, SP and S1L increased of 24.2%, 19.64%, and 12.82% respectively from day 1 to day 7. For BM-MSC, the activity increased of 21%, 15.77% and 15.95% respectively on SB, SP and S1L from day 1 to day 7. Although cell metabolic activities were improved both for WJ-MSC and BM-MSC from day 1 to day 7, the cell metabolic activities decreased as the surface treatment went from SB to SP and S1L, especially for WJ-MSC.

MSC morphology and location on the scaffold

The morphology of MSCs on the scaffold by SEM (Fig.6) showed that cells gathered to form cell sheets between fibers, and also indicated ECM synthesis. Fluorescent images (Fig.7) displayed a spindle and elongated shape of MSCs along the fibers. MSCs

tended to grow along the fiber direction in a homogeneous manner, migrated and proliferated across fibers to form cell bridges. Quantification of morphological changes of nucleus induced by scaffolds is illustrated in Fig.8. Mean nuclear area of WJ-MSC (224.7 μm^2) was smaller ($p < 0.05$) than BM-MSC (246.9 μm^2) on tissue culture polystyrene (TCPS). For WJ-MSC, the mean nuclear area did not change between cells on scaffold and cells on TCPS. In contrast, for BM-MSC, the mean nuclear area decreased for cells on SB and S1L compared to cell nucleus on TCPS. The nuclear aspect ratio (length/width) of cells significantly increased ($p < 0.05$) comparing to cell nucleus on TCPS for both WJ-MSC and BM-MSC.

Extracellular matrix expression by MSC on the scaffold

Results concerning collagen and tenascin-C expression are shown in Fig.9. Green points on the scaffold correspond to collagen type I, collagen type III and tenascin-C synthesized by WJ-MSC and BM-MSC respectively on day 14. It was observed that both types of collagens and tenascin-C were substantially secreted, independently of the surface modification.

Chemotactic properties of scaffold on MSC

Cell migration was performed to evaluate the effect of scaffold and scaffold modification on MSCs chemotaxis. As observed on fluorescent images showed in Fig.10, the number of migrated BM-MSC tended to be higher than WJ-MSC induced by SB, SP and S1L, and this was confirmed by fluorescent intensity. It also demonstrated that MSCs chemotaxis was most activated under the stimulation of S1L

for WJ-MSC and BM-MSC by fluorescent spectrophotometer.

DISCUSSION

PLCL[31] is an elastomeric synthetic copolymer combining biocompatible, degradable PLLA and PCL, resulting in desirable mechanical properties. It is of great interest in tissue engineering,[14,32] because of its biocompatibility, biodegradability, and easy-processing. Vuornos et al[33] compared a foamed PLCL(70/30) structure with a braided poly(L/D)lactide (PLA, 96L/4D) scaffold for tendon tissue engineering, and PLCL was judged to be excessively elastic to form a braided structure in their study. On the contrary, our group developed a controllable method to fabricate a uniform, porous, braided structure based on elastic PLCL (85/15). Noteworthy, the number of fiber layers could be adjusted to fulfill the mechanical requirements of different ligaments. Moreover, PLL/HA layer-by-layer system was reported to be one of the classical PEM for cell attachment, proliferation and ECM synthesis in many works.[24, 25] In our study, we introduced PLL/HA PEM on a braided PLCL scaffold for the first time and confirmed by FTIR that PLL and HA were deposited on the surface of PLCL fibers[29, 30, 34]. After the replacement of PLL by PLL-FITC, the fluorescence intensity was increased from SP to S1L by CLSM. A polygonal and particle-like structure of PLL and HA were additionally detected on scaffold by AFM.

The interaction between cells and biomaterials is influenced[35] by physicochemical properties of scaffold (surface topography, surface toughness, wettability, stiffness, and crystallinity), and also cell sources. PLL/HA modification could therefore influence the

scaffold surface microenvironment[36] as local mechanical, wettability, toughness and so on. In a non-reported preliminary study, we firstly compared the deposition order of PLL and HA by testing cell metabolic activity, and the results demonstrated that PLL constitutes a cell-adhesive layer while HA is cell-repellent layer. PLL/HA polyelectrolyte films have been previously reported[36] to be a pH-responsive PEM, and both pH6.0-6.5 and pH7.4 have been applied for PLL/HA bilayer deposition prior to the present study[24, 36]. Based on these published data, the effects of pH (pH6.3 and pH7.4) on PEM deposition was assessed and different PLL/HA bilayers numbers were compared (reported in supplementary material) in order to optimize LBL modification on scaffold for both WJ-MSC and BM-MSC. As a result, for both MSCs, cell proliferation did not increase over one layer modification. Moreover, pH 6.3 for PEM deposition greatly encouraged MSCs metabolic activity, especially for WJ-MSC (reported in supplementary material). Consequently, in the present contribution, SB, SP and S1L made in pH6.3 were selected.

Cell attachment, proliferation, ECM synthesis and migration are a series of prerequisite activities for tissue regeneration. It is also modulated by bioactive molecular such as growth factors. In the present study, MSCs attached well on scaffolds as shown by the formation of cell sheets. There was no significant difference of cell attachment between non-modified and modified scaffolds. Cell cytoskeleton organization has been previously reported[37] to relate to cell fate on scaffold, to be beneficial to predict cell commitment, and it also indicates cell senescence. Senescent

mesenchymal stem cells were characterized with enlarged, irregular morphology, following with the decrease of phenotype and differentiation abilities[38]. Fluorescent images reported in the present study presented a spindle-shape cell cytoskeleton covering the fibers. The nuclear size and shape were also related to the physiological process[39] as cell senescence, differentiation, and diseases. The quantitative data of cell nuclear morphology indicated an elongated and relatively spindle-like nuclear shape with decreased nuclear area while increased aspect ratio for WJ-MSC and BM-MSC on scaffold than on TCPS. Cells grew along the longitudinal direction of the fibers which could be an adaptable, resistant cell-scaffold system to response to mechanical stimulation. The results of Alamar Blue assay indicated that cell proliferated well on scaffold, and the metabolic activity did not show significant change after PLL/HA scaffold modification for WJ-MSC or for BM-MSC. Collagen constitutes the main component of native ligament tissue[40], and its high expression is a basic requirement for the formation of ligament-like extracellular matrix. In addition, Tenascin-C has been shown to be a promising specific indicator[41] of ligament ECM, and it has been reported[42] to be highly expressed in regenerative process of musculoskeletal tissue, and to provide elasticity to tissues in reaction to heavy tensile loading. In the present study, Collagen I, collagen III and tenascin-C were secreted by BM-MSC and WJ-MSC on the scaffold within 14 days, which could have been encouraged by ascorbic acid in the medium. This pointed out that BM-MSC-scaffold and WJ-MSC-scaffold had potential in the future to form ligamentous tissue. Additionally,

other specific indicators as tenomodulin and scleraxis could have been characterized, especially during a long-term culture including mechanical or biological stimulation. Cell migration is a crucial step in the tissue healing process since cells firstly migrate to the injury site or target area. Consequently, migration was assessed in present study and our results showed that chemotaxis of WJ-MSC and BM-MSC was activated by SB, SP and S1L. This migration was even more pronounced for one layer scaffold, compared to SB and SP. This may show a possibility to recruit MSC for *in vivo* implantation. These cell-scaffold constructs showed satisfying biocompatibility, and the effect of growth factors incorporation into this PEM layer will be assessed in the forthcoming developments.

CONCLUSION

A PLCL braided scaffold with PLL/HA modification was designed in our study. The mechanical, morphological and biological results concerning the activity of WJ-MSC and BM-MSC and the ECM synthesis showed that it may constitute a promising scaffold for ligament tissue engineering. The incorporation of LBL increased cell chemotaxis, which opens interesting perspectives for *in vivo* application. In the future, the developed LBL technology will be used to incorporate growth factors on PLCL braided scaffold in order to encourage tissue growth and the regeneration of a functional ligamentous tissue.

REFERENCE

1. Khan W. Ligament tissue engineering. Regen Strateg Treat Knee Jt Disabil.

Springer; 2017.
2. Barber JG, Handorf AM, Allee TJ, Li W-J. Braided nanofibrous scaffold for tendon and ligament tissue engineering. Tissue Eng Part A. 2011;19:1265–1274.
3. Ge Z, Yang F, Goh JC, Ramakrishna S, Lee EH. Biomaterials and scaffolds for ligament tissue engineering. J Biomed Mater Res A. 2006;77:639–652.
4. Leong NL, Petrigliano FA, McAllister DR. Current tissue engineering strategies in anterior cruciate ligament reconstruction. J Biomed Mater Res A. 2014;102:1614–24.
5. Lavoie P, Fletcher J, Duval N. Patient satisfaction needs as related to knee stability and objective findings after ACL reconstruction using the LARS artificial ligament. The Knee. 2000;7:157–63.
6. Samuelsson K, Andersson D, Karlsson J. Treatment of Anterior Cruciate Ligament Injuries With Special Reference to Graft Type and Surgical Technique: An Assessment of Randomized Controlled Trials. Arthrosc J Arthrosc Relat Surg. 2009;25:1139–74.
7. Laurencin CT, Freeman JW. Ligament tissue engineering: An evolutionary materials science approach. Biomaterials. 2005;26:7530–6.
8. Yagi M, Kuroda R, Nagamune K, Yoshiya S, Kurosaka M. Double-bundle ACL reconstruction can improve rotational stability. Clin Orthop. 2007;454:100–107.
9. Kaeding CC, Aros B, Pedroza A, Pifel E, Amendola A, Andrish JT, Dunn WR, Marx RG, McCarty EC, Parker RD. Allograft versus autograft anterior cruciate ligament reconstruction: predictors of failure from a MOON prospective longitudinal cohort. Sports Health. 2011;3:73–81.
10. Carlisle JC, Parker RD, Matava MJ. Technical considerations in revision anterior cruciate ligament surgery. J Knee Surg. 2007;20:312–322.
11. Guarino V, Causa F, Ambrosio L. Bioactive scaffolds for bone and ligament tissue. Expert Rev Med Devices. 2007;4:405–418.
12. Yang S, Leong K-F, Du Z, Chua C-K. The design of scaffolds for use in tissue engineering. Part I. Traditional factors. Tissue Eng. 2001;7:679–689.
13. Cooper JA, Lu HH, Ko FK, Freeman JW, Laurencin CT. Fiber-based tissue-engineered scaffold for ligament replacement: design considerations and in vitro evaluation. Biomaterials. 2005;26:1523–32.
14. Laurent CP, Vaquette C, Martin C, Guedon E, Wu X, Delconte A, Dumas D, Hupont S, Isla ND, Rahouadj R. Towards a tissue-engineered ligament: Design and preliminary evaluation of a dedicated multi-chamber tension-torsion bioreactor. Processes. 2014;2:167–179.
15. Laurent CP, Ganghoffer J-F, Babin J, Six J-L, Wang X, Rahouadj R. Morphological characterization of a novel scaffold for anterior cruciate ligament tissue engineering. J Biomech Eng. 2011;133:065001.
16. Lee J, Guarino V, Gloria A, Ambrosio L, Tae G, Kim YH, Jung Y, Kim S-H, Kim SH. Regeneration of Achilles' tendon: the role of dynamic stimulation for

enhanced cell proliferation and mechanical properties. J Biomater Sci Polym Ed. 2010;21:1173–1190.
17. Ge Z, Goh JCH, Lee EH. Selection of cell source for ligament tissue engineering. Cell Transplant. 2005;14:573–583.
18. Chen J, Altman GH, Karageorgiou V, Horan R, Collette A, Volloch V, Colabro T, Kaplan DL. Human bone marrow stromal cell and ligament fibroblast responses on RGD-modified silk fibers. J Biomed Mater Res A. 2003;67:559–570.
19. Cooper JA, Bailey LO, Carter JN, Castiglioni CE, Kofron MD, Ko FK, Laurencin CT. Evaluation of the anterior cruciate ligament, medial collateral ligament, achilles tendon and patellar tendon as cell sources for tissue-engineered ligament. Biomaterials. 2006;27:2747–2754.
20. Van Eijk F, Saris D b. f., Riesle J, Willems W j., van Blitterswijk C a., Verbout A j., Dhert W j. a. Tissue Engineering of Ligaments: A Comparison of Bone Marrow Stromal Cells, Anterior Cruciate Ligament, and Skin Fibroblasts as Cell Source. Tissue Eng. 2004;10:893–903.
21. Tang Z, Wang Y, Podsiadlo P, Kotov NA. Biomedical applications of layer-by-layer assembly: from biomimetics to tissue engineering. Adv Mater. 2006;18:3203–3224.
22. Costa RR, Mano JF. Polyelectrolyte multilayered assemblies in biomedical technologies. Chem Soc Rev. 2014;43:3453–3479.
23. Sahoo S, Toh SL, Goh JC. A bFGF-releasing silk/PLGA-based biohybrid scaffold for ligament/tendon tissue engineering using mesenchymal progenitor cells. Biomaterials. 2010;31:2990–2998.
24. Yamanlar S, Sant S, Boudou T, Picart C, Khademhosseini A. Surface functionalization of hyaluronic acid hydrogels by polyelectrolyte multilayer films. Biomaterials. 2011;32:5590–5599.
25. Hahn SK, Hoffman AS. Characterization of biocompatible polyelectrolyte complex multilayer of hyaluronic acid and poly-L-lysine. Biotechnol Bioprocess Eng. 2004;9:179–183.
26. Pavesio A, Renier D, Cassinelli C, Morra M. Anti-adhesive surfaces through hyaluronan coatings. Med Device Technol. 1997;8:20–1, 24–7.
27. Huang W-M, Gibson SJ, Facer P, Gu J, Polak JM. Improved section adhesion for immunocytochemistry using high molecular weight polymers of L-lysine as a slide coating. Histochemistry. 1983;77:275–279.
28. Zhang D, Zhang Y, Zheng L, Zhan Y, He L. Graphene oxide/poly-l-lysine assembled layer for adhesion and electrochemical impedance detection of leukemia K562 cancercells. Biosens Bioelectron. 2013;42:112–118.
29. Kalpan G, Shalini VS, Jonnalagadda S, Kumar N. Fast degradable poly (L-lactide-co-e-caprolactone) microspheres for tissue engineering: synthesis, characterization, and degradation behavior. J Polym Sci A1. 2007;45:2755–2764.
30. Xu J, Zhang J, Gao W, Liang H, Wang H, Li J. Preparation of chitosan/PLA blend

micro/nanofibers by electrospinning. Mater Lett. 2009;63:658–660.
31. Jeong SI, Kim B-S, Kang SW, Kwon JH, Lee YM, Kim SH, Kim YH. In vivo biocompatibilty and degradation behavior of elastic poly(l-lactide-co-ε-caprolactone) scaffolds. Biomaterials. 2004;25:5939–46.
32. Vaquette C, Kahn C, Frochot C, Nouvel C, Six J-L, De Isla N, Luo L-H, Cooper-White J, Rahouadj R, Wang X. Aligned poly(L-lactic-co-e-caprolactone) electrospun microfibers and knitted structure: A novel composite scaffold for ligament tissue engineering. J Biomed Mater Res A. 2010;94A:1270–82.
33. Vuornos K, Björninen M, Talvitie E, Paakinaho K, Kellomäki M, Huhtala H, Miettinen S, Seppänen-Kaijansinkko R, Haimi S. Human adipose stem cells differentiated on braided polylactide scaffolds is a potential approach for tendon tissue engineering. Tissue Eng Part A. 2016;22:513–523.
34. Amorim S, Martins A, Neves NM, Reis RL, Pires RA. Hyaluronic acid/poly-L-lysine bilayered silica nanoparticles enhance the osteogenic differentiation of human mesenchymal stem cells. J Mater Chem B. 2014;2:6939–6946.
35. Lutolf MP, Hubbell JA. Synthetic biomaterials as instructive extracellular microenvironments for morphogenesis in tissue engineering. Nat Biotechnol. 2005;23.
36. Burke SE, Barrett CJ. pH-Responsive Properties of Multilayered Poly(l-lysine)/Hyaluronic Acid Surfaces. Biomacromolecules. 2003;4:1773–83.
37. Treiser MD, Yang EH, Gordonov S, Cohen DM, Androulakis IP, Kohn J, Chen CS, Moghe PV. Cytoskeleton-based forecasting of stem cell lineage fates. Proc Natl Acad Sci. 2010;107:610–615.
38. Wagner W, Horn P, Castoldi M, Diehlmann A, Bork S, Saffrich R, Benes V, Blake J, Pfister S, Eckstein V, Ho AD. Replicative Senescence of Mesenchymal Stem Cells: A Continuous and Organized Process. PLOS ONE. 2008;3:e2213.
39. Chen B, Co C, Ho C-C. Cell shape dependent regulation of nuclear morphology. Biomaterials. 2015;67:129–36.
40. Altman G, Horan R, Martin I, Farhadi J, Stark P, Volloch V, Vunjak-Novakovic G, Richmond J, Kaplan DL. Cell differentiation by mechanical stress. FASEB J. 2002;16:270–2.
41. Altman GH, Horan RL, Lu HH, Moreau J, Martin I, Richmond JC, Kaplan DL. Silk matrix for tissue engineered anterior cruciate ligaments. Biomaterials. 2002;23:4131–41.
42. Jarvinen TAH. Mechanical loading regulates the expression of tenascin-C in the myotendinous junction and tendon but does not induce de novo synthesis in the skeletal muscle. J Cell Sci. 2003;116:857–66.

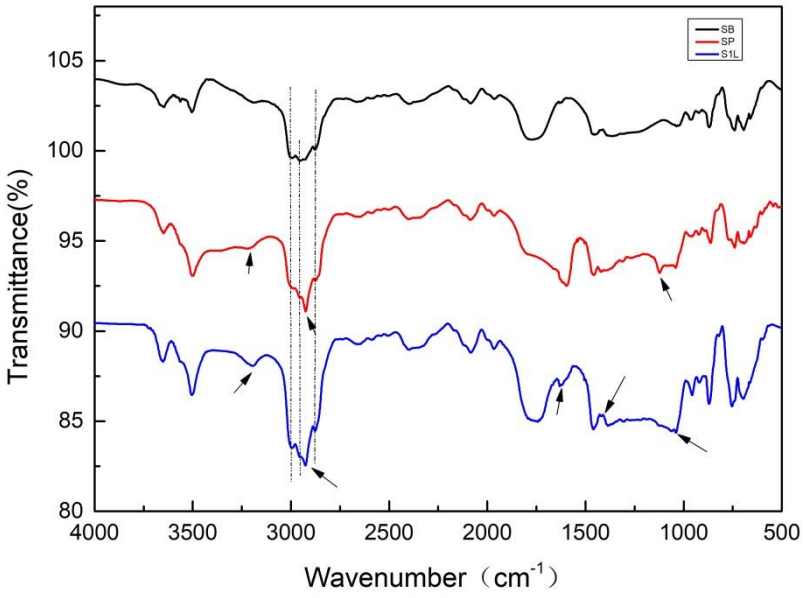

Fig1. FTIR of PLL/HA modified on PLCL scaffold (SB:PLCL scaffold blank, SP: PLCL-PLL, S1L: PLCL-PLL/HA-PLL).

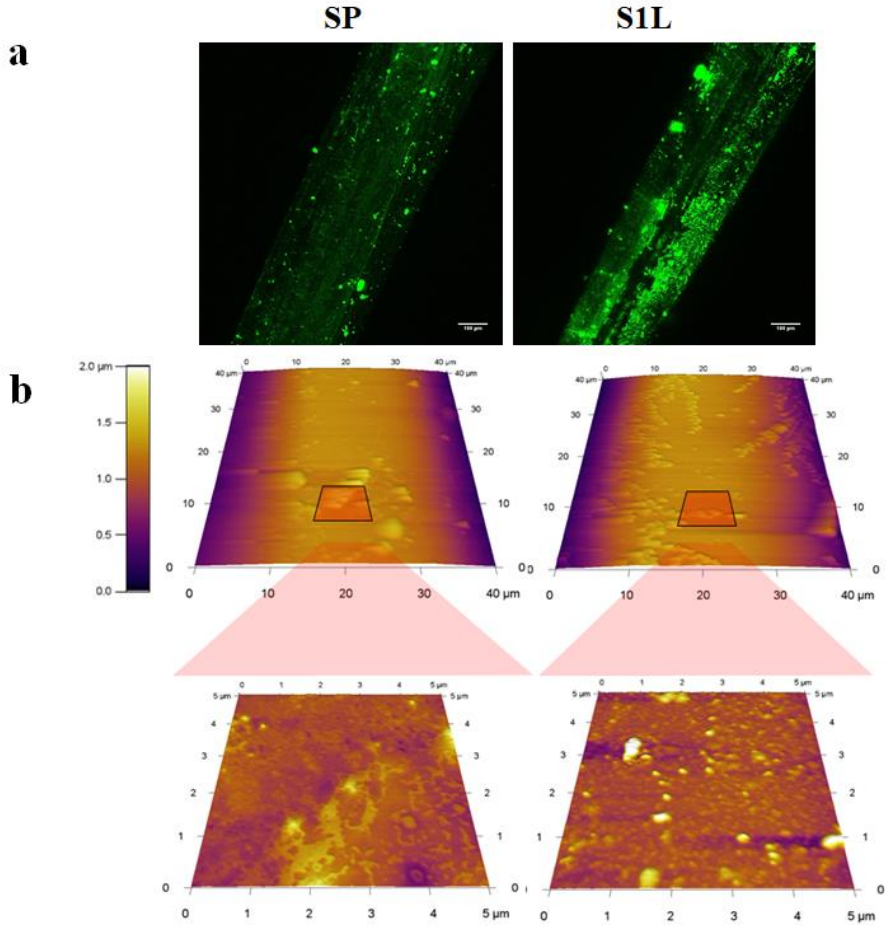

Fig2. Morphology of PLL-FITC/HA on PLCL fiber by CLSM (a), and topology of PLL/HA on PLCL fiber by AFM (b).(SP: PLCL scaffold-PLL-FITC, S1L: PLCL scaffold-PLL/HA-PLL).

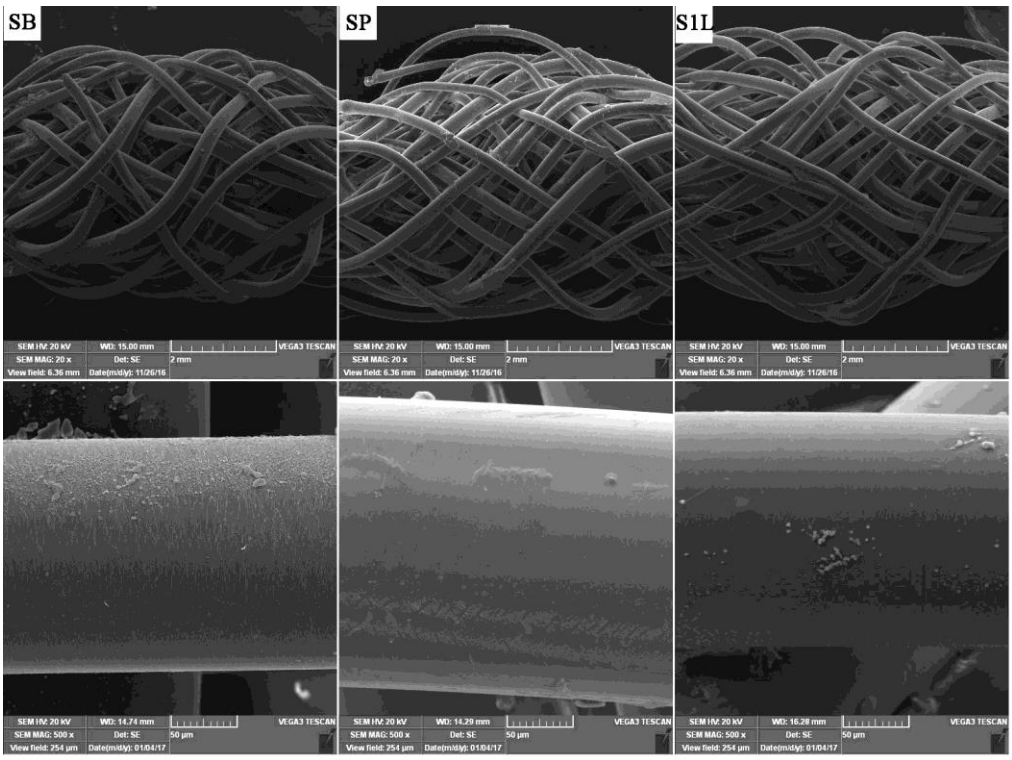

Fig3. Morphology of PLCL scaffold and PLCL scaffold modified with PLL/HA by SEM. (SB:PLCL scaffold blank, SP: PLCL-PLL, S1L: PLCL-PLL/HA-PLL).

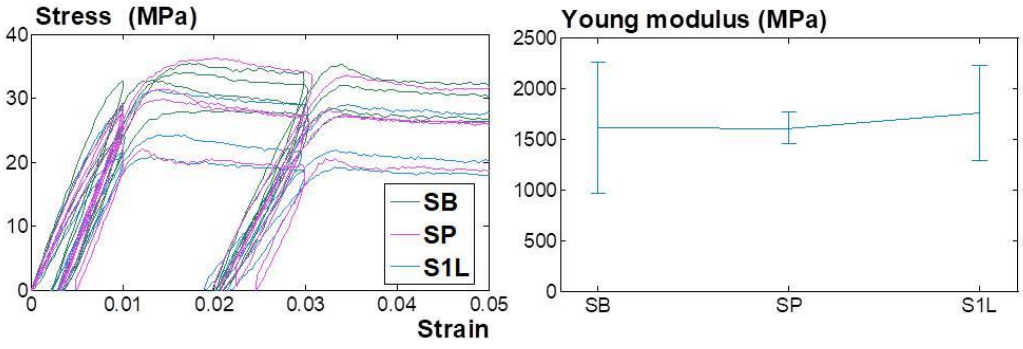

Fig4. Mechanical test of PLCL fibers (SB:PLCL fiber blank, SP: PLCL fiber-PLL, S1L: PLCL fiber-PLL/HA-PLL).

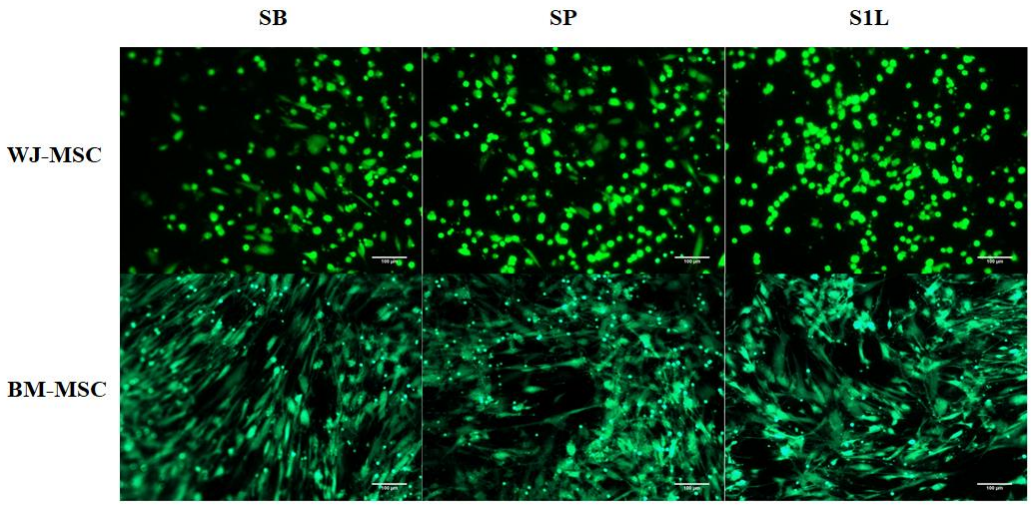

Fig5. Migration of WJ-MSC and BM-MSC induced by PLCL scaffold, scaffold-PLL and scaffold- PLL/HA-PLL.

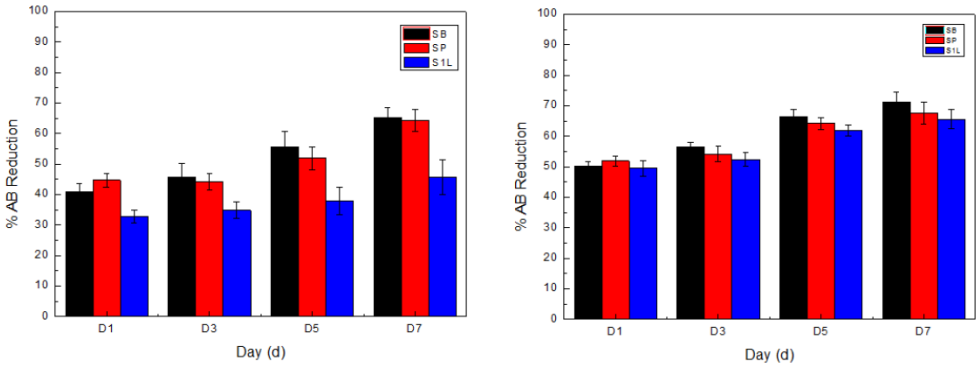

Fig6. Reduction of AB of WJ-MSC and BM-MSC on PLCL scaffold (SB:PLCL scaffold blank, SP: PLCL-PLL, S1L: PLCL-PLL/HA-PLL).

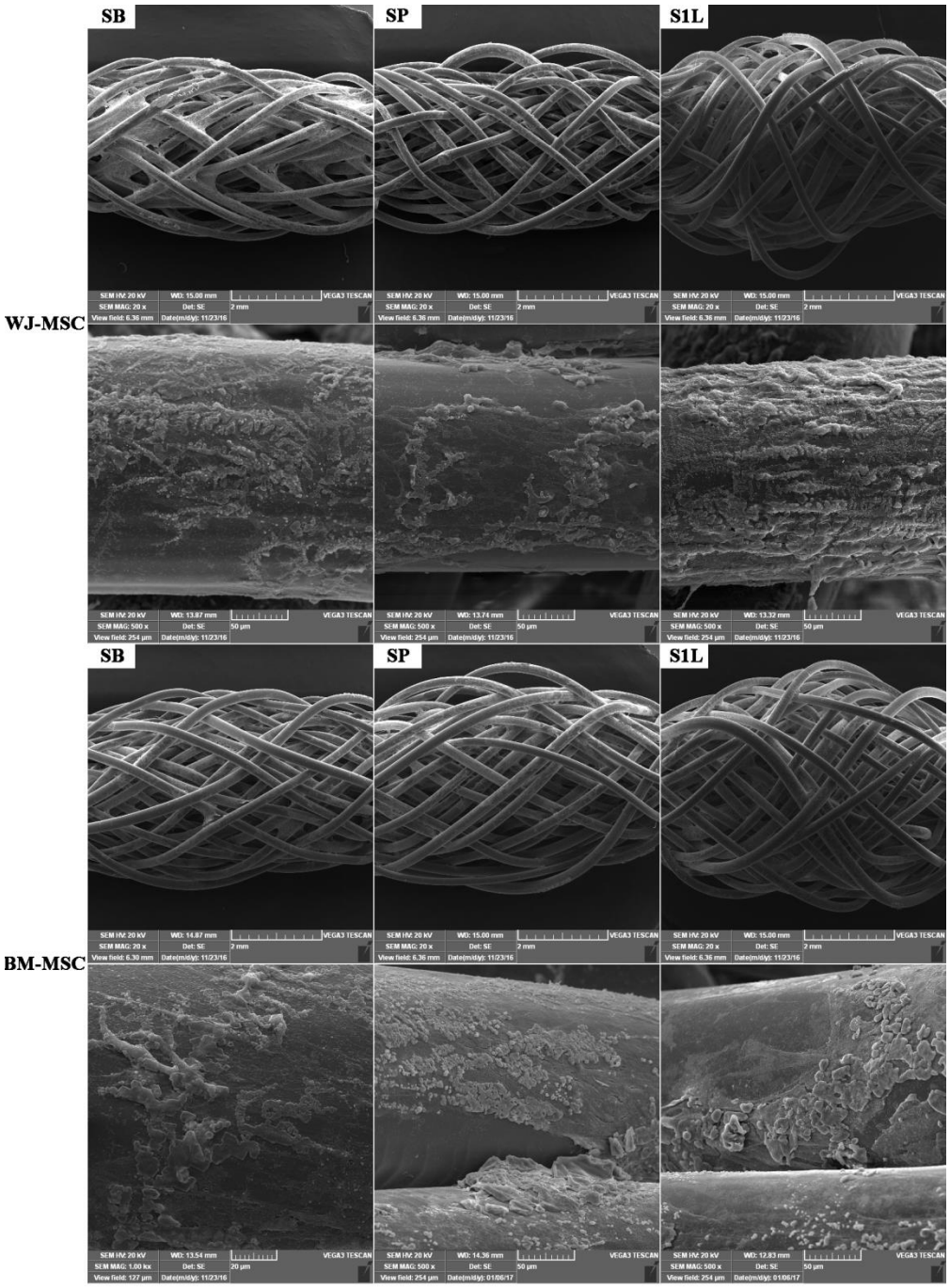

Fig7. Morphology and distribution of WJ-MSC and BM-MSC on scaffold by SEM. (SB:PLCL scaffold blank, SP: PLCL-PLL, S1L: PLCL-PLL/HA-PLL).

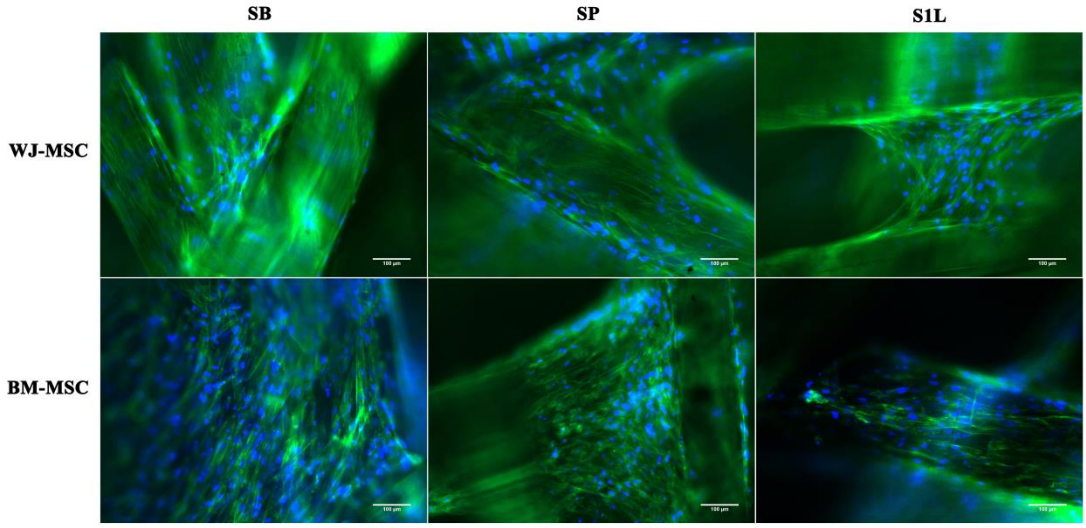

Fig8. Morphology and distribution of WJ-MSC and BM-MSC on scaffold by florescence microscopy.(SB: PLCL scaffold blank, SP: PLCL-PLL, S1L: PLCL-PLL/HA-PLL).

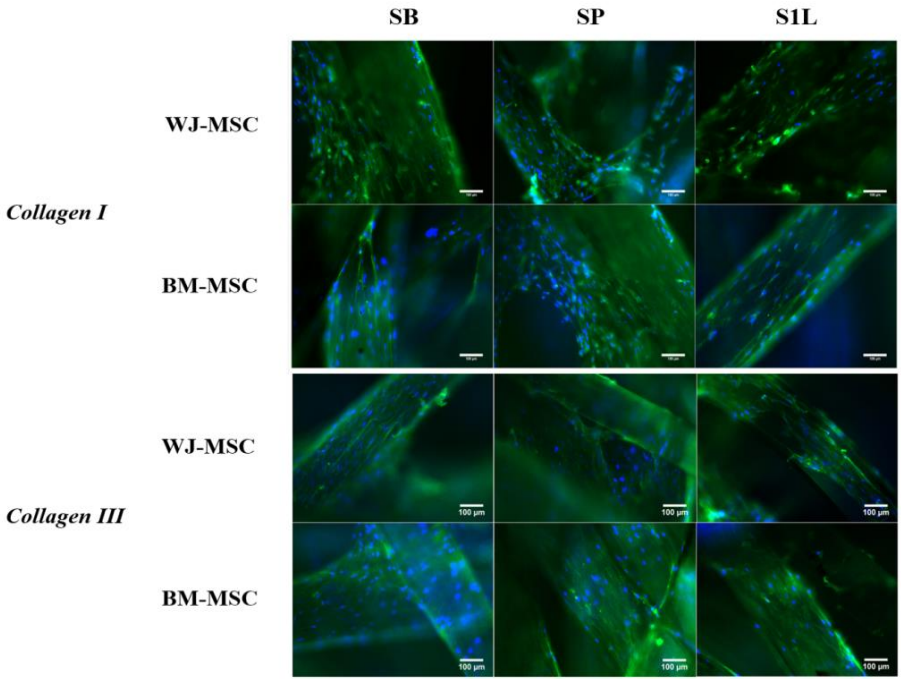

Fig9. Collagen I and collagen III expression by WJ-MSC and BM-MSC on PLCL scaffolds on D14. (SB:PLCL scaffold blank, SP: PLCL-PLL, S1L: PLCL-PLL/HA-PLL).